ELSEVIER

Journal of Alloys and Compounds 446–447 (2007) 23–27

Journal of ALLOYS AND COMPOUNDS

www.elsevier.com/locate/jallcom

First principles screening of destabilized metal hydrides for high capacity H_2 storage using scandium

Sudhakar V. Alapati [a], J. Karl Johnson [b,c], David S. Sholl [a,c,*]

[a] *Department of Chemical Engineering, Carnegie Mellon University, Pittsburgh, PA 15213, USA*
[b] *Department of Chemical and Petroleum Engineering, University of Pittsburgh, Pittsburgh, PA 15261, USA*
[c] *National Energy Technology Laboratory, Pittsburgh, PA 15236, USA*

Received 15 September 2006; received in revised form 19 October 2006; accepted 25 October 2006
Available online 29 December 2006

Abstract

Favorable thermodynamics are a prerequisite for practical H_2 storage materials for vehicular applications. Destabilization of metal hydrides is a versatile route to finding materials that reversibly store large quantities of H_2. First principles calculations have proven to be a useful tool for screening large numbers of potential destabilization reactions when tabulated thermodynamic data are unavailable. We have used first principles calculations to screen potential destabilization schemes that involve Sc-containing compounds. Our calculations use a two-stage strategy in which reactions are initially assessed based on their reaction enthalpy alone, followed by more detailed free energy calculations for promising reactions. Our calculations indicate that mixtures of $ScH_2 + 2LiBH_4$, which will release 8.9 wt.% H_2 at completion and will have an equilibrium pressure of 1 bar at around 330 K, making this compound a promising target for experimental study. Along with thermodynamics, favorable kinetics are also of enormous importance for practical usage of these materials. Experiments would help identify possible kinetic barriers and modify them by developing suitable catalysts.

Keywords: Metal hydrides; Hydrogen absorbing materials; Thermodynamic properties; Computer simulations

1. Introduction

The challenges of finding materials that can be used for high capacity, reversible storage of H_2 for mobile applications are well known [1–5]. Among the multiple criteria that must be satisfied by any potential material for these applications are the capacity requirements of reversibly storing in the vicinity of 6.5 wt.% H_2 and >80 kg H_2/m^3 on a system basis and the need for full reversibility at moderate temperatures (preferably <150 °C). Simple metal hydrides such as MgH_2 (7.7 wt.% H_2) and LiH (12.7 wt.% H_2) have the potential to satisfy the capacity requirements, but are so thermodynamically stable that elevated temperatures are required to release H_2. A powerful and general route for addressing this stability issue was introduced recently by Vajo et al. [6,7]. This approach uses physical mixtures of metal hydrides and other compounds of light elements to improve the thermodynamics of H_2 release relative to direct metal hydride decomposition. In one example introduced by Vajo et al., the reaction of $2MgH_2 + Si \rightarrow Mg_2Si + 2H_2$ releases 5.0 wt.% H_2 at completion with equilibrium pressures that are at least four times greater than that for MgH_2 decomposition at room temperature [7]. Since the initial work of Vajo et al., a number of destabilized reactions involving compounds such as $LiBH_4$ and $LiNH_2$ have been studied experimentally [8–11].

The concept of using destabilization to alter the reaction thermodynamics of metal hydrides is quite general, and a very large number of potential reaction schemes exist. A key challenge in this area is therefore to identify promising reactions from this large pool of possible reactions. A small number of reactions can be examined using tabulated thermodynamic data [12,13]. For the great majority of possible reactions, however, the thermodynamic data necessary for this analysis are not currently available. We have shown previously that first principles calculations are an efficient and accurate means of predicting the thermodynamic data needed to assess potential destabilized reaction schemes. In our previous work, we have used this approach to screen more than one hundred potential reactions involving stoichiometric compounds of Al, B, Li, Ca, H, Mg, N, and Si [14].

* Corresponding author.
E-mail address: sholl@andrew.cmu.edu (D.S. Sholl).

0925-8388/$ – see front matter © 2006 Elsevier B.V. All rights reserved.
doi:10.1016/j.jallcom.2006.10.166

In this paper, we use first principles methods to consider whether ScH_2 might be a useful component in destabilized reaction schemes for H_2 storage. Initially, ScH_2 may appear to be rather unpromising, since it only stores 4.3 wt.% H_2 and it is extremely stable; the experimentally observed reaction enthalpy for decomposition was estimated to be 201 and 258 kJ/mol H_2 by different groups [15–18]. Hydrogen adsorption by Laves phase alloys formed by Sc and heavier elements such as Ni, Co, Mn, and Cr have been studied previously by Akiba and co-workers [19]. We know of no previous results, however, for H_2 uptake or release for combinations of ScH_2 and other light metal hydrides. Our calculations suggest that ScH_2 can be combined with other light metal hydrides to yield reactions with promising properties.

Our analysis below, as in our earlier work, is based purely on the thermodynamics of reactions of interest [14,20]. The kinetics of these reactions is, of course, also of enormous importance in any practical application. Our focus on thermodynamics is driven by the observation that, at least in principle, reaction kinetics can be improved using appropriate catalysts, control of particle size, etc. Favorable reaction thermodynamics, in contrast, are a prerequisite for meeting the operational guidelines for mobile applications mentioned above.

2. Computational methods

Detailed descriptions of using plane wave DFT calculations to examine candidate destabilized reaction schemes for H_2 storage are available in our earlier work [14,20]. Briefly, we performed calculations using the Vienna ab initio Simulation Package (VASP) using the Perdew-Wang 91 GGA functional [21–23]. The PAW method was used for all calculations [24]. In our initial calculations, we optimized the structure of a variety of solid materials. Total energy calculations for each material were performed using an $8 \times 8 \times 8$ Monkhorst-Pack mesh of k-points and geometries were relaxed until the forces on all atoms were less than 0.03 eV/Å. These structural optimization calculations were initialized using data from Wycoff [25], Pearson's Handbook [26], and the ICSD database [27]. An energy cutoff of 425 eV was used for the final total energy calculations, and this cutoff was increased by 30% during geometry optimization to obtain a reliable stress tensor.

An initial characterization of the thermodynamics of reversible H_2 storage in each candidate reaction was calculated by using DFT results to compute the enthalpy of the reaction at 0 K from

$$\Delta H_0 = \sum_{\text{products}} E - \sum_{\text{reactants}} E, \quad (1)$$

Here, E is the total energy of one of the bulk structures of interest or of gaseous H_2 as calculated by DFT. This formulation does not account for zero point energy corrections or other vibrational contributions to free energy, but we have shown before that ΔH_0 is a useful quantity to remove reactions with highly unfavorable reaction thermodynamics from further consideration [14,20].

For selected reactions, we performed additional calculations to assess the temperature-dependent free energy of reaction [20]. This requires calculation of the phonon density of states and the resulting vibrational contributions to the free energy for each material involved in a reaction. For solid materials, these calculations were performed using the PHONON code developed by Parlinski [28] using the same exchange-correlation functional and energy cutoff as for our total energy calculations. Force constants were computed using displacements of individual atoms of 0.05 Å. In these calculations, the number of k-points was chosen so that the density of k-points in k-space was approximately equal to the mesh used for our total energy calculations. The analogous results for gaseous H_2 have been described previously [20].

Once the reaction free energy has been computed for a reaction of interest, it is straightforward to construct the van't

Table 1
Lattice parameters and space groups for Sc-containing compounds as listed in the ICSD database [27] and computed using DFT

Compound	Space group	Structural parameters (Å)	
		Experimental	Calculated
Al	$Fm\bar{3}m$	$a = 4.049$	$a = 4.05$
Al_2Sc	$Fd\bar{3}mS$	$a = 7.58$	$a = 7.58$
Al_3Sc	$Pm\bar{3}m$	$a = 4.105$	$a = 4.11$
AlSc	$Pm\bar{3}m$	$a = 3.45$	$a = 3.37$
$AlSc_2$	$P63/mmc$	$a = 4.888$, $c = 6.166$	$a = 4.88$, $c = 6.14$
Li_3ScN_2	$Ia\bar{3}$	$a = 10.045$	$a = 10.04$
$LiBH_4$	$Pnma$	$a = 7.173$, $b = 4.434$, $c = 6.798$	$a = 7.13$, $b = 4.32$, $c = 6.57$
$LiBH_4$	$P6_3mc$	$a = 4.276$, $c = 6.948$	$a = 4.17$, $c = 7.26$
LiH	$Fm\bar{3}m$	$a = 4.085$	$a = 3.94$
Sc	$P63/mmc$	$a = 3.308$, $c = 5.2653$	$a = 3.29$, $c = 5.11$
Sc_5Si_3	$P63/mcm$	$a = 7.861$, $c = 5.812$	$a = 7.87$, $c = 5.80$
ScB_2	$P6/mmm$	$a = 3.1478$, $c = 3.5169$	$a = 3.14$, $c = 3.52$
ScB_{12}	$Fm\bar{3}m$	$a = 7.402$	$a = 7.40$
ScH_2	$Fm\bar{3}m$	$a = 4.78$	$a = 4.75$
ScN	$Fm\bar{3}m$	$a = 4.44$	$a = 4.49$
ScSi	$Cmcm$	$a = 3.988$, $b = 9.882$, $c = 3.659$	$a = 3.98$, $b = 9.88$, $c = 3.67$
$ScSi_2$	$P6/mmm$	$a = 3.66$, c = 3.87	$a = 4.02$, $c = 3.62$
Si	$Fd\bar{3}m$	$a = 5.430$	$a = 5.46$

Hoff plot for that reaction [7,20]. Because the example presented below involves $LiBH_4$, it is important to note that $LiBH_4$ undergoes a phase transition from an orthorhombic phase to a hexagonal phase at 381 K. This phase change has been incorporated in our calculations following the method detailed in our previous work [20].

3. Results

We performed DFT calculations for all Sc-containing compounds comprised from light elements that are listed in the Wycoff [25], Pearson's Handbook [26] and the ICSD database [27]. The DFT-optimized structural parameters for these compounds, and several other compounds relevant to our approach, are compared with experimental data in Table 1. This list extends the larger set of compounds not containing Sc that we have considered previously [14]. The agreement between the DFT results and experiment is generally very good as expected. $ScSi_2$ is a layered compound that is likely to have significant van der Waals contributions to its interlayer spacings. As a result, it is not surprising that DFT does not make precise predictions for the structure of this material. Similar results have been seen before for other layered compounds such as graphite and MoS_2 [29].

3.1. Screening using first principles reaction enthalpies

Table 2 lists 12 reactions involving ScH_2 that can be considered using combinations of the materials listed in Table 1. Apart from the direct decomposition of ScH_2, no previous thermodynamic data are available for these reactions. Most of these reactions release relatively small amounts of H_2 at completion, but there are several that involve more than 6.5 wt.% H_2. We have arbitrarily chosen 6.5 wt.% as a cutoff for screening purposes. The first stage of our computational screening process is to compare our computed 0 K reaction enthalpies, ΔH_0, with the range of reaction enthalpies that can generate equilibrium pressures of 1 bar in the temperature range 300–450 K. These enthalpy ranges are based on the limited range of reaction entropies that

Table 2
DFT-calculated reaction enthalpies at 0 K for possible destabilized reactions involving ScH_2, with all energies given in kJ/mol H_2

Reaction	H_2 (wt.%)	ΔH_0
$ScH_2 + 3Al \rightarrow Al_3Sc + H_2$	1.58	19.6
$ScH_2 + 2Si \rightarrow ScSi_2 + H_2$	1.95	95.5
$ScH_2 + 2Al \rightarrow Al_2Sc + H_2$	2.00	57.9
$ScH_2 + Si \rightarrow ScSi + H_2$	2.68	39.8
$ScH_2 + Al \rightarrow AlSc + H_2$	2.73	111.1
$5ScH_2 + 3Si \rightarrow Sc_5Si_3 + 5H_2$	3.16	81.9
$2ScH_2 + Al \rightarrow AlSc_2 + 2H_2$	3.33	148.0
$ScH_2 \rightarrow Sc + H_2$	4.29	200.0
$ScH_2 + LiNH_2 \rightarrow ScN + LiH + 1.5H_2$	4.32	−43.8
$2ScH_2 + 3LiNH_2 \rightarrow Li_3ScN_2 + ScN + 5H_2$	6.19	11.3
$ScH_2 + 2LiBH_4 \rightarrow ScB_2 + 2LiH + 4H_2$	8.91	49.7
$ScH_2 + 12LiBH_4 \rightarrow ScB_{12} + 12LiH + 19H_2$	12.42	74.1

Calculations involving $LiBH_4$ are based on *ortho*-$LiBH_4$.

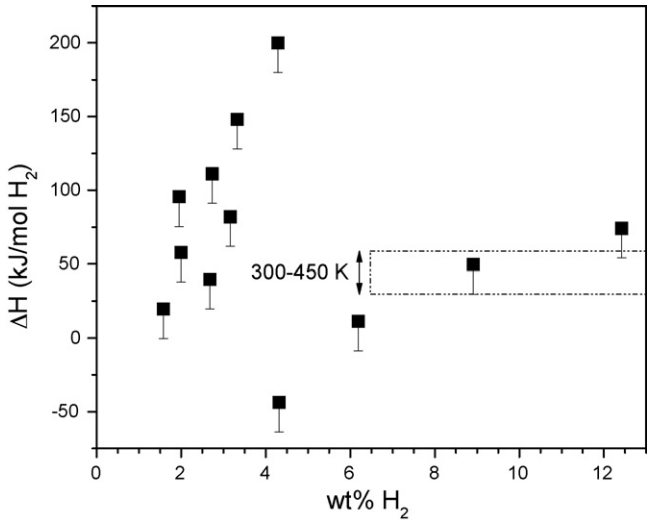

Fig. 1. Screening plot for reactions involving ScH_2. For details, see the text.

are observed in a large collection of metal hydride decomposition reactions [20]. This process is shown in Fig. 1. In this figure, the filled symbols are the ΔH_0 values arising from our DFT calculations, and the vertical bars indicate the range of zero point energy corrections that we have observed in a previous analysis of destabilized metal hydride reactions [20]. Interpreting this screening plot is straightforward; only those reactions that lie within the rectangular region bounded by the dashed lines (including the vertical bars) have the potential to have acceptable gravimetric capacity and reaction thermodynamics. The height of the rectangular box is an estimate of the range of enthalpies required to result in a vapor pressure of 1 bar within a given temperature range.

It is not surprising that almost all the reactions involving ScH_2 we have considered in Fig. 1 hold little promise for high capacity reversible storage of H_2. The positive outcome of this screening exercise, however, is that two reactions are predicted to have favorable properties. The first of these is

$$ScH_2 + 2LiBH_4 \rightarrow ScB_2 + 2LiH + 4H_2, \quad (2)$$

a reaction that releases 8.91 wt.% H_2 on completion. On a volumetric basis, this reaction stores 98.9 kg H_2/m^3. This reaction is analogous to the destabilization of $LiBH_4$ with MgH_2 that has been studied experimentally by Vajo et al. [6]. The calculated heat of reaction for Eq. (2) is $\Delta H_0 = 49.7$ kJ/mol H_2 based on *ortho*-$LiBH_4$.

The second promising reaction identified in Fig. 1 also involves ScH_2 and $LiBH_4$. In this case, $ScH_2 + 12LiBH_4 \rightarrow ScB_{12} + 12LiH + 19H_2$, we calculated $\Delta H_0 = 74.1$ kJ/mol H_2 using *ortho*-$LiBH_4$. This enthalpy is only marginally smaller than the DFT-computed enthalpy for direct decomposition of $LiBH_4$ [14,30,31]. More importantly, this result suggests that these reaction products are more likely to initially react to form ScB_2 via Eq. (2) until the ScH_2 is consumed. On this basis, we exclude the reaction forming ScB_{12} from further consideration.

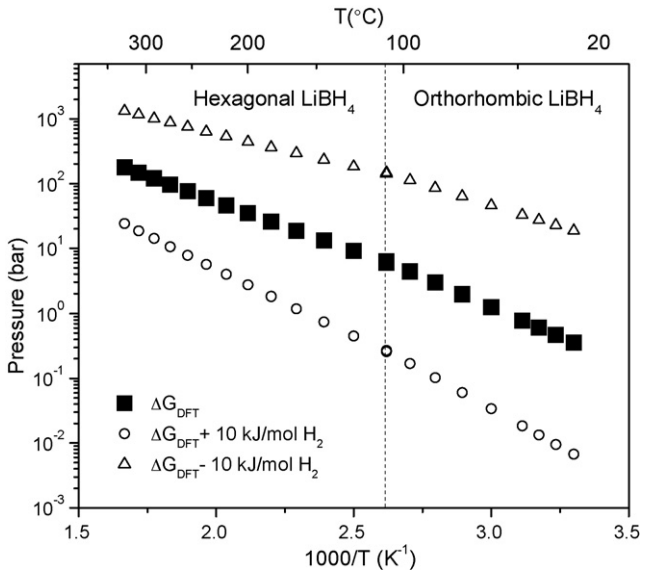

Fig. 2. van't Hoff plot from DFT calculations for $ScH_2 + 2LiBH_4 \rightarrow ScB_2 + 2LiH + 4H_2$. The open symbols represent estimates for the uncertainty in the calculations. For details, see the text.

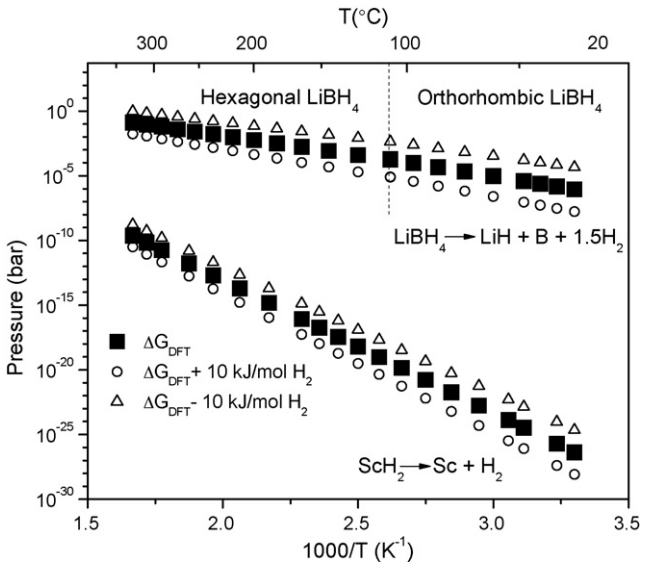

Fig. 3. van't Hoff plot from DFT calculations for $ScH_2 \rightarrow Sc + H_2$ and $LiBH_4 \rightarrow LiH + B + 1.5H_2$. For details, see the text.

3.2. Screening using first princples reaction free energies

The analysis shown in Fig. 1 is based on estimating ranges for reaction entropies and zero point energy corrections from previous detailed studies of metal hydride decomposition reactions [14,20,32]. While this approach is useful for reducing the number of potential reactions that must be examined in detail, it is clearly useful to obtain more detailed information on the reaction free energy for any promising reactions. In particular, we performed free energy calculations for Eq. (2). As described in Section 2; we approached this task by computing the vibrational density of states for each of the solid materials involved in the reaction within the harmonic approximation [33]. These calculations allow the zero point energies, temperature dependent vibrational contributions, and entropies of each material to be calculated.

Our calculations for Eq. (2) give a reaction enthalpy and entropy at 300 K of $\Delta H_{300} = 34.1$ kJ/mol H_2 and $\Delta S_{300} = 105.7$ J/K/mol H_2. The fact that the reaction enthalpy at 300 K is smaller than the result given above for ΔH_0 is due largely to zero point energy effects [20]. The calculated reaction entropy is very similar to the value seen for other destabilized metal hydride reactions and lies within the bounds used to construct to regions with desirable material properties in Fig. 1 [20].

The van't Hoff plot for Eq. (2) based on our DFT calculations is shown in Fig. 2. In this figure, results are shown for both phases of $LiBH_4$ as appropriate for the experimentally observed phase transition temperature for this material [34]. We have previously compared calculations of this type with experimental data for a variety of metal hydrides [20]. This comparison shows that DFT predictions are fully consistent with available experimental data if an uncertainty of ± 10 kJ/mol H_2 is associated with the DFT-computed reaction free energies. The open symbols in Fig. 2 show the van't Hoff results arising from these uncertainties. Even given this uncertainty, the van't Hoff plot in Fig. 2 is extremely promising. Our DFT calculations predict that the equilibrium pressure for this reaction is 1 bar at around 330 K, which is very favorable for practical hydrogen storage applications.

To emphasize the crucial role of destabilization in the reaction discussed above, we have shown the DFT-computed van't Hoff plot for the direct decomposition of ScH_2 in Fig. 3. This reaction has a predicted equilibrium pressure of $\sim 10^{-27}$ bar at room temperature. Figure 3 also shows the DFT-computed van't Hoff plot for direct decomposition of $LiBH_4$. At room temperature the decomposition of $LiBH_4$ to form LiH and B results in an equilibrium pressure of $\sim 10^{-7}$ bar. The effect of destabilization can clearly be seen when ScH_2 and $LiBH_4$ react together to form ScB_2 and LiH, with a calculated equilibrium pressure of 0.3 bar at room temperature.

4. Conclusion

Destabilized reactions for H_2 storage involving Sc based compounds have been screened with DFT calculations. Many of these reactions will not be of practical interest because of low H_2 content or unfavorable thermodynamics. We have, however, been able to identify one reaction with favorable thermodynamics and a theoretical H_2 capacity of 8.91 wt.%. Our calculations indicate that this reaction has an equilibrium pressure of 1 bar at 330 K, which makes it promising for hydrogen storage applications. Experimental work on this compound is needed to test our predictions.

Acknowledgements

This work was supported by the DOE grant number DE-FC36-05G015066 and performed in conjunction with the DOE Metal Hydride Center of Excellence. JKJ and DSS are NETL Faculty Fellows.

References

[1] L. Schlapbach, A. Züttel, Nature 414 (2001) 353.
[2] National Hydrogen Energy Roadmap, US Department of Energy, http://www.eere.energy.gov/hydrogenandfuelcells/pdfs/hydrogen_posture_plan.pdf, 2002, p. 17.
[3] DOE Hydrogen Storage Targets, http://www.eere.energy.gov/hydrogenandfuelcells/mypp/pdfs/storage.pdf.
[4] A Multiyear Plan for the Hydrogen R&D Program: Rationale, Structure, and Technology Roadmaps, US Department of Energy, http://www.eere.energy.gov/hydrogenandfuelcells/pdfs/bk28424.pdf, 1999, p. 32.
[5] A. Züttel, Mater. Today 6 (2003) 24.
[6] J.J. Vajo, S.L. Skeith, F. Meters, J. Phys. Chem. B 109 (2005) 3719.
[7] J.J. Vajo, F. Mertens, C.C. Ahn, C. Robert, J. Bowman, B. Fultz, J. Phys. Chem. B 108 (2004) 13977.
[8] P. Chen, Z. Xiong, J. Luo, J. Lin, K.L. Tan, J. Phys. Chem. B 107 (2003) 10967.
[9] P. Chen, Z. Xiong, J. Luo, J. Lin, K.L. Tan, Nature 420 (2002) 302.
[10] M. Aoki, K. Miwa, T. Noritake, G. Kitahara, Y. Nakamori, S. Orimo, S. Towata, Appl. Phys. A 80 (2005) 1409.
[11] F.E. Pinkerton, G.P. Meisner, M.S. Meyer, M.P. Balogh, M.D. Kundrat, J. Phys. Chem. B 109 (2005) 6.
[12] IEA/DOE/SNL, Hydride Databases available at Hydride Information Center, Sandia National Laboratories, http://hydpark.ca.sandia.gov.
[13] NIST Chemistry Webbook, NIST Standard Reference Database Number 69, in: P.J. Linstrom, W.G. Mallard (Eds.), National Institute of Standards and Technology, Gaithersburh MD, 2005, p. 20889.
[14] S.V. Alapati, J.K. Johnson, D.S. Sholl, J. Phys. Chem. B 110 (2006) 8769.
[15] J.F. Stampfer, The Scandium Hydrogen System, Los Alamos Sci. Lab. Report, LA-3473, 1966.
[16] M.L. Lieberman, P.G. Wahlbeck, J. Phys. Chem. 69 (1965) 3514.
[17] W.M. Mueller, J.P. Blackledge, G.G. Libowitz, Metal Hydrides, Academic Press, New York, NY, 1968.
[18] F.D. Manchester (Ed.), Phase Diagrams of Binary Hydrogen Alloys, ASM International, Materials Park, OH, c2000.
[19] M. Yoshida, H. Ishibashi, K. Susa, T. Ogura, E. Akiba, J. Alloys Compd. 226 (1995) 161.
[20] S.V. Alapati, J.K. Johnson, D.S. Sholl, J. Phys. Chem. B, in press.
[21] G. Kresse, J. Hafner, Phys. Rev. B 47 (1993) 558.
[22] G. Kresse, J. Furthmüller, Phys. Rev. B 54 (1996) 11169.
[23] J.P. Perdew, J.A. Chevary, S.H. Vosko, K.A. Jackson, M.R. Pederson, D.J. Singh, C. Fiolhais, Phys. Rev. B 46 (1992) 6671.
[24] G. Kresse, D. Joubert, Phys. Rev. B 59 (1758).
[25] R.W.G. Wycoff, The Structure of Crystals, The Chemical Catalog Company Inc., New York, 1931.
[26] P. Villars, Pearson's Handbook: Crystallographic Data for Intermetallic Phases, Desk ed., ASM International, Materials Park, OH, 1997.
[27] The Inorganic Crystal Structure Database (ICSD), http://www.fiz-informationsdienste.de/en/DB/icsd/.
[28] K. Parlinski, Software PHONON, 2005.
[29] D. Sorescu, D.S. Sholl, A. Cugini, J. Phys. Chem. B 107 (2003) 1988.
[30] T.J. Frankcombe, G.-J. Kroes, A. Züttel, Chem. Phys. Lett. 405 (2005) 73.
[31] K. Miwa, N. Ohba, S. Towata, Y. Nakamori, S. Orimo, Phys. Rev. B 69 (2004) 245120.
[32] W. Grochala, P.P. Edwards, Chem. Rev. 104 (2004) 1283.
[33] G.J. Ackland, J. Phys.: Condens. Matter 14 (2000) 2975.
[34] J.-P. Soulié, G. Renaudin, R. Icrný, K. Yvon, J. Alloys Compd. 346 (2002) 200.